

Gravitational-Wave Emission from Rotating Gravitational Collapse

Richard F. Stark

Center for Radiophysics and Space Research, Cornell University, Ithaca, New York 14853

and

Tsvi Piran

Racah Institute of Physics, The Hebrew University, Jerusalem, Israel, and The Institute for Advanced Study, Princeton, New Jersey 08540

(Received 13 May 1985)

We present results for the gravitational radiation from the collapse to a black hole of rotating relativistic polytropes. The wave form closely resembles that emitted by a test particle infalling into a black hole, but the amplitude is reduced and opposite in sign. Less than 0.07% of the star's mass is converted to gravitational-wave energy. With sufficient rotation, the star bounces and no black hole forms. These results were obtained with a fully general-relativistic computer code that evolves rotating axisymmetric configurations and directly computes their gravitational-radiation emission.

PACS numbers: 95.30.Sf, 04.30.+x, 97.60.-s

The complexity of the Einstein equations has, until now, limited the calculation of the gravitational radiation from gravitational collapse to either approximate perturbation results,¹ or numerical methods applied to unrealistic configurations.^{2,3} As a result, estimates for the emission of gravitational radiation from a rotating stellar collapse have been wildly uncertain. We report here numerical results for this gravitational radiation obtained with a general-relativistic code which evolves general axisymmetric configurations (either matter or vacuum initial data) by solving the complete coupled Einstein and hydrodynamic equations, and directly evaluates the resulting gravitational emission at large radii. The particular collapse we present (that of a ro-

tating polytropic star) is not meant to model a realistic stellar collapse (this requiring still uncertain astrophysics).¹ Nevertheless, most of the gravitational-radiation emission in a collapse to a black hole occurs late into the collapse (when the collapsing configuration has dimensions less than 2 Schwarzschild radii) when pressure and other microphysical effects no longer dominate, so that our results can be expected to be at least representative of such an event, provided axial symmetry is maintained.

We solve the "3 + 1" form of the Einstein equations in which the spatial metric, h_{ij} , and the extrinsic curvature, K_i^j , are evolved from one selected spatial hypersurface to another. We use the radial gauge suggested by Bardeen and Piran.⁴ The four-dimensional metric has the form

$$ds^2 = -(N^2 - N^i N_i) dt^2 - 2N_i dx^i dt + h_{rr}^2 dr^2 + r^2 d\theta^2 / (1 + \eta) + r^2 (1 + \eta) \sin^2 \theta d\phi + \xi d\theta)^2$$

with t the time label, N the lapse, and N^i the shift vector. The foliation we use consists of a combination of polar and maximal slicing. There are many advantages to this choice of gauge.⁴⁻⁶ A key point is that two of the evolved gravitational field variables— η and ξ —tend to the transverse traceless gravitational-wave amplitudes h_+ and h_\times at large radii. This allows a direct determination of the gravitational wave form.⁵ The gravitational emission is so small that only a carefully devised scheme is able to detect it numerically.⁷

We solve seventeen coupled partial differential equations in the three coordinates (t , r , and θ) for twelve geometrical variables (h_{rr} , η , ξ ; five components of K_i^j , N , and N^i) and five hydrodynamic variables (the density, thermal energy density, and momentum density). We use the numerical scheme described by Bardeen and Piran.⁴ This scheme is partially constrained (the Hamiltonian constraint is solved for h_{rr} , η , ξ , and K_i^j are evolved). The evolved value

of h_{rr} and the momentum constraints are used as checks. The code, which will be described in detail elsewhere,⁸ is second-order accurate and employs a staggered-variable grid with grid velocity.^{2,3,6,8,9} Each timestep takes 0.15-sec central-processor-unit time on a Cray-1 for a grid of 80×16 radial by angular points,⁸⁻¹² and 3000–5000 time steps are required for the results we describe here.

It is essential that a code of this kind be shown to pass rigorous testing. We have performed an extensive series of tests which can be broadly classified into general stability tests, hydrodynamic tests, conservation tests, and comparison tests with known perturbation solutions. These tests include the following: (i) Evolution of the vacuum Schwarzschild exterior ($r > 2M$) for many gravitational times. (ii) Propagation of gravitational waves (for both polarizations) along inward and outward characteristics with negligi-

ble reflection at the outer boundary. Evolution to flat space-time for low-amplitude waves, and black-hole formation for high initial wave amplitudes. (iii) Stable evolution of initial data consisting of flat space-time plus a small-amplitude "random data" superimposed. (iv) Evolution of stable extreme relativistic polytropes for many free-fall time scales. This included checking the excitation of the lowest radial mode oscillations for adiabatic indices $\Gamma > \Gamma_{\text{crit}}$, as well as the instability to collapse for $\Gamma < \Gamma_{\text{crit}}$ [with $\Gamma_{\text{crit}} = \frac{4}{3} +$ (general-relativistic corrections)].¹³ (v) Conservation of the Arnowitt-Deser-Misner mass, total angular momentum, and the specific angular momentum spectrum. (vi) Propagation of generalized linearized Teukolsky waves¹⁴ for both polarization modes. (vii) Comparison of the gravitational-wave emission from the infall of a spheroidal dust shell onto a Schwarzschild black hole with known perturbation results^{15,16} (Fig. 1). (viii) Comparison of the gravitational-wave emission and hydrodynamics for uniformly rotating homogeneous spheroidal collapse with known Newtonian plus quadrupole-formalism results.¹⁸ These tests will be discussed in detail elsewhere.⁸

Here we present results¹⁰⁻¹² for the collapse of a polytropic star with adiabatic index $\Gamma = 2$. The initial configuration is that of a spherically symmetric (relativistic) polytrope with a radius of $6GM/c^2$ (M being the mass of the star)¹⁹ which then undergoes a pressure reduction to a chosen fraction f_p (with $f_p = 0.01$ or 0.4) of its equilibrium pressure; simultaneously, the star is given an angular momentum distribution approximating rigid-body rotation. The total angular momentum J of the star is measured by the dimensionless parameter $a = J/(GM^2/c)$. With the chosen equation of state, all properties of the collapse scale in an elementary fashion with M . Our initial configuration has a central density $1.9 \times 10^{15} (M/M_\odot)^{-2} \text{ g cm}^{-3}$ and radius $8.8 \times 10^5 M/M_\odot \text{ cm}$.

The nature of the collapse depends on the value of a . For $a < a_{\text{crit}}$, with a_{crit} near unity ($a_{\text{crit}} = 1.2 \pm 0.2$ for $f_p = 0.01$ and for $f_p = 0.4 a_{\text{crit}} = 0.80 \pm 0.05$), collapse proceeds to a black hole. For $a < 0.5$ the collapse proceeds in an almost spherically symmetric fashion with only small rotational flattening of the star. The meridional component of the velocity points very nearly radially inwards throughout the collapse, and the matter falls in without any shocks forming. After a time of $25M$ for $f_p = 0.01$ ($35M$ for $f_p = 0.4$) the central lapse drops to below 10^{-10} and in the region $r < 2M$, the lapse very quickly becomes and remains below 10^{-10} indicating black-hole formation.²⁰ During this time the central proper density grows by a factor of 75 for $f_p = 0.01$ (15 for $f_p = 0.4$) until its value freezes because of the collapse of the lapse, while matter outside this frozen region continues to fall in. For $0.5 < a < a_{\text{crit}}$, the rotational effects on the col-

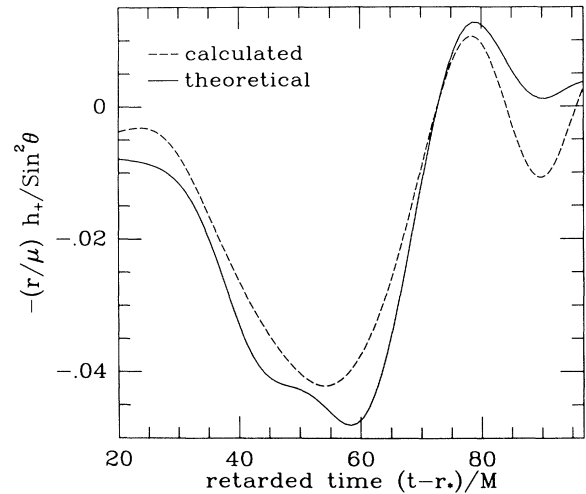


FIG. 1. Comparison test for the wave form (Ref. 16) from a spheroidal dust shell (mass μ and at $t=0$ homogeneous with inner and outer polar radii $12M$ and $20M$ and eccentricity 0.55) infalling into a Schwarzschild black hole (mass $M \gg \mu$). The amplitude is only 1/10 that from a test particle (Ref. 17).

lapsing matter become noticeable. The collapsing configuration becomes significantly nonspherical, showing considerable flattening into the equator. The time for the central lapse to collapse increases with a , during which the central density increases similarly as for smaller a . The star, having flattened towards the equator, bounces vertically from the equator while continuing to collapse inwards. For $f_p = 0.01$, the lapse collapses and freezes the star while it is highly flattened. For $f_p = 0.4$ the lapse collapses later, and the star is able to become more spherical again before freezing. In spite of the flattening of the star, the collapsed region with lapse $< 10^{-10}$ remains nearly spherical, its radius decreasing with increasing a (e.g., for $a = 0.9$ it is $1.4M$). When $a > a_{\text{crit}}$, rotational effects dominate and prevent black-hole formation (the lapse now remaining near unity everywhere).²¹ Material near the equator starts to expand radially outwards (apart from the very inner region, for the smaller a in this interval, which moves initially inwards). Matter near the pole collapses towards the equator but moves radially outwards while doing so. These motions are eventually halted and turned around as the star bounces. The star then oscillates about a flattened equilibrium structure. The highly rotating configurations show maxima in their coordinate density somewhat displaced from the origin (and in the equatorial plane).

The gravitational emission for the collapse is monitored at the outer edge of the grid ($50M$ from the origin) as well as at smaller radii. Figures 2(a) and 2(b)

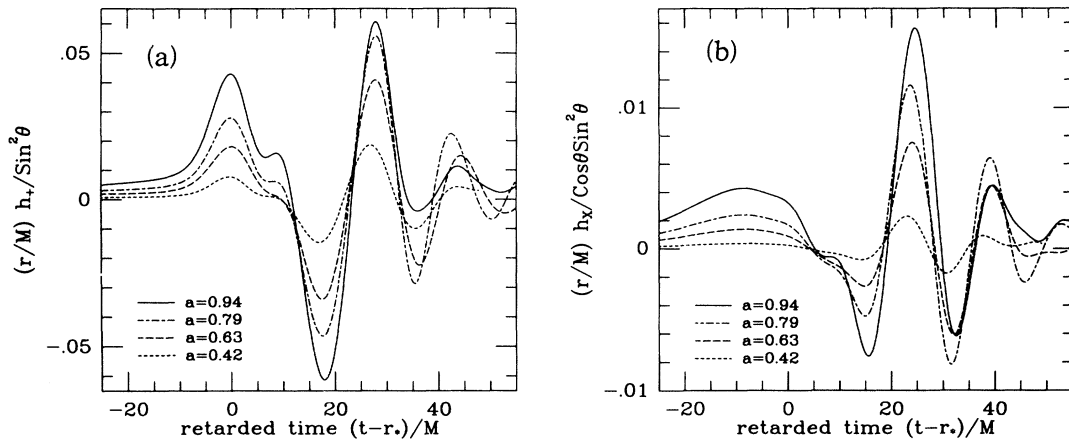


FIG. 2. (a) Plus and (b) cross mode wave forms for the collapse to a black hole by stars ($f_p = 0.01$) of various angular momenta a .

show the transverse traceless amplitudes of the two polarization modes h_+ and h_x for black-hole collapse ($a < a_{crit}$) for $f_p = 0.01$. The general shape of the wave form remains much the same over the entire range²² of a while the amplitude increases with a . Results for $f_p = 0.4$ are similar, although later in retarded time. The maximum plus-mode amplitude is closely

$$|(r/M)h_+|_{max} = \min\{0.1a^2, A_{max}\} \quad (0 < a < a_{crit}),$$

where $A_{max} = 0.06$ for $f_p = 0.01$, and $A_{max} = 0.025$ for $f_p = 0.4$. The wave form is remarkably similar to that of a single particle falling into a black hole,¹⁷ the amplitude for our case only being smaller and opposite in sign. The decrease in amplitude from the single-particle case is due to phase cancellation of emission from the extended regions of the star (seen also in recent perturbation studies).^{15, 16, 23} The relative minus sign occurs because the equatorially flattened collapsing configuration is crudely approximating to a collapsing sphere (which does not radiate) minus material near the pole. Our results are closely similar also to those of perturbation studies of collapsing stars.^{16, 24} As in the single-particle case, most of the gravitational-wave emission arises at a retarded time when the dimensions of the star are between $2M$ and $4M$ and the emission is then red shifted while propagating to large distances. The wave forms settle to nearly their asymptotic forms at fairly small radii ($r \sim 25M$) as they propagate outwards. As expected for axisymmetric configurations, the amplitude of the cross polarization mode is always < 0.2 that of the even mode. The emission in the plus mode is dominantly quadrupolar with the expected $\sin^2\theta$ angular dependence. (The smaller-amplitude cross mode has the expected $\cos\theta\sin^2\theta$ angular dependence.) The power spectrum of these wave forms peaks in the

frequency range $(0.035-0.08)(GM/c^3)^{-1}\text{Hz}$ [i.e., $(7-16)(M/M_\odot)^{-1}\text{kHz}$; wavelengths of $12M-28M$].

The energy emitted in this gravitational radiation (Fig. 3) clearly indicates a very low efficiency for this emission. Less than 7×10^{-4} of the asymptotic mass is converted into gravitational radiation. (The numerical result for $a = 0$ is $\Delta E/Mc^2 = 10^{-8}$ thus demonstrating the numerical accuracy of the code.) The energy emitted scales as a^4 for low a (found also in perturbation and other approximate studies^{15-18, 24}), and levels off as a nears a_{crit} . These results closely follow

$$\Delta E/Mc^2 = \min\{1.4 \times 10^{-3}a^4, \epsilon_{max}\} \quad (0 < a < a_{crit}),$$

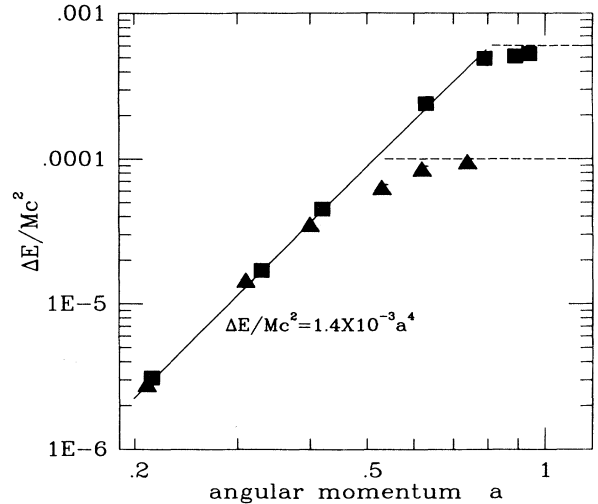


FIG. 3. Energy of the gravitational-wave emission from the collapse to a black hole by stars (squares $f_p = 0.01$; triangles $f_p = 0.4$) of various angular momenta a . Solid line fits the a^4 scaling; dashed lines mark ϵ_{max} .

where $\epsilon_{\max} = 6 \times 10^{-4}$ for $f_p = 0.01$ and $\epsilon_{\max} = 1 \times 10^{-4}$ for $f_p = 0.4$. In all cases, the energy of emission in the plus mode exceeds by at least a factor of 10 that in the cross mode.

For $a_{\text{crit}} < a < 2$, when no black hole forms, the wave form has the form of several sharp peaks about the retarded time of stellar bounce, superimposed on a slowly varying envelope. The corresponding energy radiated is $\Delta E/Mc^2 = 10^{-3}$ for $f_p = 0.01$ (10^{-4} for $f_p = 0.4$). However, unlike the black-hole results,²² these results depend significantly on the particular choice of initial model used.

In conclusion, we have shown the efficiency of gravitational-wave emission from the collapse of an axisymmetric rotating polytrope to a black hole to be very low ($\Delta E/Mc^2 < 7 \times 10^{-4}$). Our h_+ wave forms are well fitted by a combination of the lowest two, $l=2$, quasinormal modes of Schwarzschild.²⁵ This, together with their similarity in shape to previous approximate computations,^{16,17,24} indicates the importance of black-hole mode excitation in determining the wave form. The insensitivity of the wave form to a reflects the weak dependence on a of the axisymmetric Kerr quasinormal-mode frequencies.²⁵ The wave-form amplitudes are determined by the details of the collapse. Results for realistic collapse to a black hole can be expected to be substantially similar provided axisymmetry is maintained. Nonaxisymmetric collapse may well be expected to increase this emission. Such a three-dimensional computation is, however, beyond the practical capabilities of present-day computers.

One of us (R.F.S.) thanks S. L. Shapiro, S. A. Teukolsky, and I. Wasserman for valuable discussions and encouragement; another (T.P.) thanks J. M. Bardeen for many conversations, remarks, and suggestions. One of us (R.F.S.) gratefully acknowledges the receipt of a Royal Society (London) Israel Academy Programme Award for 1981-83 at the Hebrew University. This work was partially supported by National Science Foundation Grant No. Phy83-05288, and Grant No. Phy84-079219.

¹For reviews, see *Gravitational Radiation*, edited by N. Deruelle and T. Piran (North-Holland, Amsterdam, 1983).

²T. Piran, Phys. Rev. Lett. **41**, 1085 (1978), and J. Comp. Phys. **35**, 254 (1980).

³J. R. Wilson, in *Sources of Gravitational Radiation*, edited by L. Smarr (Cambridge Univ. Press, England, 1979); C. R. Evans, in *Numerical Astrophysics*, edited by J. M. Centrella,

J. M. LeBlanc, and R. L. Bowers (Jones and Bartlett, Boston, 1985).

⁴J. M. Bardeen and T. Piran, Phys. Rep. **96**, 205 (1983).

⁵J. M. Bardeen, in Ref. 1.

⁶T. Piran, in Ref. 1.

⁷T. Nakamura, Prog. Theor. Phys. **65**, 1876 (1981), employed a gauge allowing the hydrodynamics but not the wave emission to be obtained from his numerical calculations.

⁸R. F. Stark and T. Piran, "A general relativistic code for rotating axisymmetric configurations and gravitational radiation: numerical methods and tests" (to be published).

⁹R. F. Stark, unpublished.

¹⁰R. F. Stark and T. Piran, "A numerical computation of gravitational wave emission from rotating gravitational collapse" (to be published).

¹¹T. Piran and R. F. Stark, in Proceedings of the Twelfth Texas Symposium on General Relativity (to be published).

¹²R. F. Stark and T. Piran, in Proceedings of the Fourth Marcel Grossmann Meeting on General Relativity (to be published).

¹³S. Chandrasekhar, Astrophys. J. **140**, 417 (1964).

¹⁴S. A. Teukolsky, Phys. Rev. D **26**, 745 (1982).

¹⁵S. L. Shapiro and I. Wasserman, Astrophys. J. **260**, 838 (1982).

¹⁶L. I. Petrich, S. L. Shapiro, and I. Wasserman, Astrophys. J., Suppl. Ser. (to be published).

¹⁷M. Davis, R. Ruffini, and J. Tiomno, Phys. Rev. D **5**, 2932 (1972).

¹⁸R. A. Saenz and S. L. Shapiro, Astrophys. J. **221**, 286 (1978).

¹⁹Preliminary wave forms for collapse from $12M$ are, for chosen a , unchanged from corresponding $6M$ results.

²⁰The radial gauge, strictly speaking, cannot identify the presence of an apparent or event horizon since, as in spherical symmetry, we expect our hypersurfaces to freeze asymptotically outside them. However, the properties of the collapsed regions which we numerically observe are consistent with those for the Kerr (black hole) solution in our gauge. This suggests that the collapsed regions are indeed those of a black hole.

²¹ a measures the *total* angular momentum. When $a_{\text{crit}} > 1$ (as may occur for nonzero initial radial infall velocity), a black hole can form from stars with $a > 1$. The black-hole spin is $a_{\text{bh}} < 1$, however, as required by cosmic censorship; the excess angular momentum is accounted for by matter surrounding the black hole.

²²The first broad peak (Fig. 2) at retarded time ~ 0 is due to the initial flattening of the star from its initial spherical configuration. This contributes little to the total energy emitted. *The rest of the wave form arises from the actual black-hole formation, and its shape is insensitive to the details of the initial configuration.*

²³T. Nakamura, Phys. Lett. B **106**, 69 (1981).

²⁴C. T. Cunningham, R. H. Price, and V. Moncrief, Astrophys. J. **224**, 643 (1978), and **230**, 870 (1979), and **236**, 674 (1980).

²⁵S. Detweiler, Astrophys. J. **239**, 292 (1980).